Borate Inhibition of Yeast Alcohol Dehydrogenase†

Katherine Woo Smith and S. L. Johnson*

ABSTRACT: Yeast alcohol dehydrogenase is inhibited competitively by borate with respect to NAD^+. An unusual mechanism of competitive inhibition prevails: the competition for the substrate NAD^+ by borate and enzyme. The following evidence supports this conclusion. (1) Much greater inhibition is observed with respect to NAD^+ as compared with NADH as substrates. (2) Borate decreases the equilibrium constant of the overall reaction in the direction of ethanol oxidation, therefore, borate enters directly into the overall reaction rather than merely decreases the effectiveness of the catalyst. (3) The K_i values for unrelated enzyme reactions are identical for NAD^+. (4) Stopped-flow experiments show burst kinetics only when NAD^+ and borate are not premixed. (5) The K_i value is identical with the inverse of the borate-NAD^+ complexation constant. (6) The pH dependence of the inhibitor demonstrates that only the $B(OH)_4^-$ species is inhibiting. These results are consistent with the preferable binding of borate to NAD^+ as compared with NADH. These two binding constants were found to be equal to 2000 ± 60 and 130 ± 8 M^{-1}, respectively. In contrast to the liver enzyme, the yeast enzyme does not show pre-steady-state burst reactions in the reduction of NAD^+. This would indicate that the interconversion of ternary complexes is at least partially rate limiting for the yeast enzyme.

Borate is known as a competitive inhibitor of pyridine nucleotide or flavin requiring enzymes. Examples are: xanthine oxidase (Roush and Norris, 1950), yeast glyceraldehyde-3-phosphate dehydrogenase (Misawa et al., 1966), yeast alcohol dehydrogenase (Weser, 1968; Roush and Gowdy, 1961), and aldehyde dehydrogenase (Deitrich, 1967).

Competitive inhibition is usually regarded as competition for the active site on the enzyme (E) by inhibitor (I) and substrate (S) as shown in eq 1a. The resulting kinetic expression is eq 1b:

$$\begin{array}{ccccc} E + S & \rightleftharpoons & ES & \longrightarrow & \text{products} \\ I \updownarrow K_i & & & & \\ EI & & & & \end{array} \qquad (1a)$$

$$v = \frac{V[S]}{K_m(1 + [I]/K_i) + [S]} \qquad (1b)$$

Since borate is known to reversibly react with NAD^+ [1] (Johnson and Smith, 1976), it is necessary to consider another mode of competitive inhibition as shown in eq 2a:

$$\begin{array}{ccccc} E + S & \rightleftharpoons & ES & \longrightarrow & \text{products} \\ I \updownarrow K_i' & & & & \\ IS & & & & \end{array} \qquad (2a)$$

In this mechanism competition for substrate by enzyme and inhibitor gives rise to an expression identical in form to eq 1b. The kinetic expression for the alternate mechanism in eq 2a is derived by substituting the concentration of the free uncomplexed substrate S, which is equal to $[S_{tot}]/(1 + [I]/K_i')$ into the Michaelis–Menten equation as shown in eq 2b. $[S_{tot}]$ is the total substrate concentration.

$$v = \frac{V[S]}{K_m + [S]} = \frac{V[S_{tot}]/(1 + [I]/K_i')}{K_m + [S_{tot}]/(1 + [I]/K_i')} = \frac{V[S_{tot}]}{K_m(1 + [I]/K_i') + [S_{tot}]} \qquad (2b)$$

The mechanisms of inhibition as described in eq 1a and 2a can be distinguished by using a dehydrogenase which fulfills two criteria: (a) steady-state kinetics under stopped-flow conditions are observed, and (b) competitive inhibition by borate is observed. It is known that the rate of the borate–pyridine nucleotide reaction can be measured using the stopped-flow technique (Johnson and Smith, 1976); therefore depending on the various premixing combinations of enzyme, inhibitor, and substrates, the initial NAD^+ will be in the unborated or borated state at the beginning of the experiment. For mechanism 2a if the NAD^+ is initially uncomplexed and enzyme is premixed with borate, shortly after mixing complexing will take place, and the velocity of the enzyme reaction will fall off accordingly. For this reason it is important that criterion (a) is followed so that the above predicted burst is not confused with a pre-steady-state burst. Yeast alcohol dehydrogenase fulfills both criteria.

Experimental Section

NAD^+ and NADH were obtained from Sigma Biochemicals. Ethanol, acetaldehyde, DL-glyceraldehyde-3-phosphoric acid (Sigma), sodium DL-lactate, and the sodium salt of L(+)-lactic acid (Sigma) were used as substrates for the enzyme reactions. Sodium borate was prepared by neutralization of boric acid with NaOH. Reagent grade sodium pyrophosphate was used for preparation of buffer solutions. Yeast alcohol dehydrogenase was purchased in its lyophilized form, yeast glyceraldehyde-3-phosphate and beef

† From the Department of Biochemistry, University of Pittsburgh School of Medicine, Pittsburgh, Pennsylvania 15261. *Received June 24, 1975.* This research is supported by Public Health Service Grant GM 16856.

[1] Abbreviations used are: YADH, yeast alcohol dehydrogenase; LADH, liver alcohol dehydrogenase; GPDH, glyceraldehyde-3-phosphate dehydrogenase; LDH, lactate dehydrogenase; NAD^+, nicotinamide adenine dinucleotide; NADH, reduced nicotinamide adenine nucleotide; B, borate; NADB, borate complex of NAD^+; NADHB, borate complex of NADH; AcCHO, acetaldehyde; NAD-SO_3^-, sulfite addition complex of NAD^+.

Table I: K_i Values for the Inhibition of Enzymes by Borate.[a]

Enzyme	K_m (NAD$^+$) ($M \times 10^{-4}$)	K_i ($M \times 10^{-4}$)	pH (±0.1)
Yeast alcohol dehydrogenase	17	4.0	9.2
	5.0 ± 1.5	5.0 ± 1.0	8.8
	3.3 ± 0.9	2.9 ± 0.5	8.4
Glyceraldehyde-3-phosphate dehydrogenase	0.91 ± 0.03	5.1 ± 1.4	8.4
Lactate dehydrogenase	0.7 ± 0.3	3.7 ± 0.6	8.4

[a] Reactions performed at 24 °C in sodium pyrophosphate buffer.

heart lactate dehydrogenases were purchased as ammonium sulfate suspensions from Sigma. The concentrations of YADH were determined at 280 nm (ϵ 1.89 × 10^5 M^{-1} cm^{-1}, Hayes and Velick, 1954). The specific activity of the enzyme was found to be 290 units/mg of protein using standard assay procedures (Vallee and Hoch, 1955). The initial rate of NADH formation was measured at 340 nm after the addition of enzyme to a 1-cm cuvette containing 26 mM PP_i buffer (pH 8.8), 0.60 M EtOH, and 1.8 mM NAD$^+$. Upon gel electrophoresis at pH 8.9 and 4°, the enzyme exhibits one major band (90%) and a more slowly migrating minor band (10%). The active site concentrations were determined by spectrophotometric titration of YADH coenzyme binding sites with NAD$^+$ in the presence of excess pyrazole, an assay procedure usually employed for LADH (Theorell and Yonetani, 1963). By this method, the normality of the enzyme-coenzyme binding capacity of a 35 μM enzyme solution was found to be 75 μN.

Steady-state rate measurements were recorded with a Cary Model 14 or a Gilford Model 240 recording spectrophotometer at 24 °C in sodium pyrophosphate buffer. Each kinetic run was initiated by the addition of substrate to a 3-ml quartz cuvette containing buffer, enzyme, and coenzyme in the absence or presence of borate. Initial rates were calculated from the changes in absorbancy at 340 nm (λ_{max}, NADH) with time. The values of K_m for NAD$^+$ or NADH and K_i for borate were obtained from Lineweaver-Burk plots (Lineweaver and Burk, 1934) of initial velocities vs. coenzyme concentrations.

The YADH-catalyzed ethanol oxidation was studied at 340 nm using a Durrum stopped-flow spectrophotometer under rapid mixing conditions (Johnson and Smith, 1976). Three premixing conditions were used: (i) NAD$^+$-borate solutions mixed with YADH-EtOH solutions; (ii) YADH-borate solutions mixed with NAD$^+$-EtOH solutions; (iii) EtOH-borate solutions mixed with NAD$^+$-YADH solutions. Reactions were performed at room temperature in 0.011 M sodium pyrophosphate, μ = 0.1 M, pH 8.7. The enzyme and NAD$^+$ concentrations used were 1.8–3.5 μM and 0.50–1.0 mM, respectively. The ethanol concentration was maintained at 0.025 M with borate concentrations being varied from 0 to 0.028 M.

The apparent equilibrium constant, K_{app}, at constant pH for the YADH-catalyzed ethanol oxidation was measured as a function of borate concentration. A Cary Model 16 spectrophotometer thermostated at 25.0 ± 0.1 °C was used for the equilibrium determinations. A pyrophosphate solution (1.5 ml), μ = 0.1 M, pH 8.7, containing 0.050 M EtOH and 0–0.056 M sodium borate is introduced into a 1-cm cuvette containing 1.5 ml of 3.5 μM enzyme and 0.0010 M NAD$^+$. Absorbance values at 340 nm are recorded for each borate concentration. From the absorbance values, NADH and the corresponding AcCHO concentrations can be determined. K_{app} can then be calculated: K_{app} = [NADH][AcCHO]/[NAD$^+$][EtOH]. In the absence of borate, K_{app} is equal to K_I, the intrinsic apparent equilibrium constant of the reaction. The values of K_I or K_{app} as a function of borate concentration were treated using a nonlinear least-squares curve fitting program on the DEC System-10 computer in order to determine the individual equilibrium constants of Scheme I.

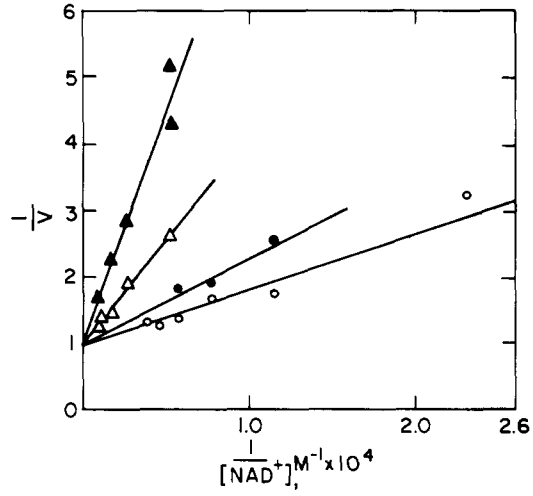

FIGURE 1: The inhibition of yeast alcohol dehydrogenase (triangles) and glyceraldehyde-3-phosphate dehydrogenase from yeast (circles) by borate in sodium pyrophosphate buffer at 24 °C and pH 8.4. (△) 1.9–11 × 10^{-4} M NAD$^+$, 0.057 M ethanol, 0.007 μM enzyme, no borate; (▲) 4.0 × 10^{-4} M sodium borate; (○) 2.2 × 10^{-5}–2.6 × 10^{-4} M NAD$^+$, 5.4 × 10^{-4} M DL-glyceraldehyde-3-phosphoric acid, 0.06 μM enzyme, no borate; (●) 4.0 × 10^{-4} M sodium borate.

Scheme I

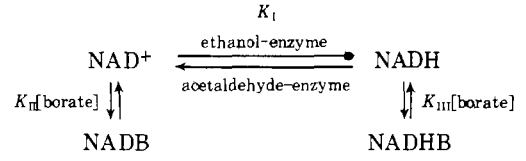

The measurement of pH of the solutions is described in the accompanying paper (Johnson and Smith, 1976).

Results

Borate competitively inhibits YADH, GPDH, and LDH with respect to NAD$^+$. The kinetics of the YADH and GPDH inhibition are shown in Figure 1. Plots of $1/v$ vs. borate show that the inhibition is linear. The values of K_i for borate and K_m for NAD$^+$ are given in Table I. The K_i values for borate inhibition are identical for YADH, GPDH, and LDH, and for YADH, is independent of pH over the pH range at which boric acid ionizes.

Borate affects not only the initial velocity of ethanol oxidation catalyzed by YADH, but also the end point of the system. The apparent equilibrium constant was measured as a function of borate concentration, the results of which are shown in Figure 2.

The rate of the reverse reaction in the presence or absence of borate, i.e., the YADH-catalyzed NADH reduction of acetaldehyde was measured under conditions in which considerable borate inhibition of the forward reaction was observed. The results in Figure 3 show much less inhibition in the reverse direction as compared with the forward

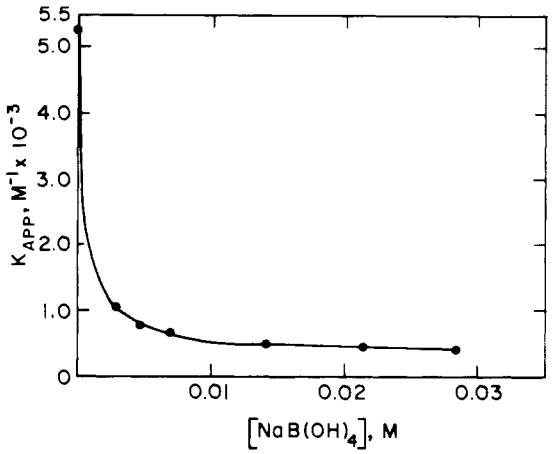

FIGURE 2: The effect of borate on the oxidation of ethanol by NAD^+ with yeast alcohol dehydrogenase at pH 8.7, 25 °C. The solid line is with K_I, K_{II}, and K_{III} equal to 0.0053, 2000, and 130 M^{-1}, respectively.

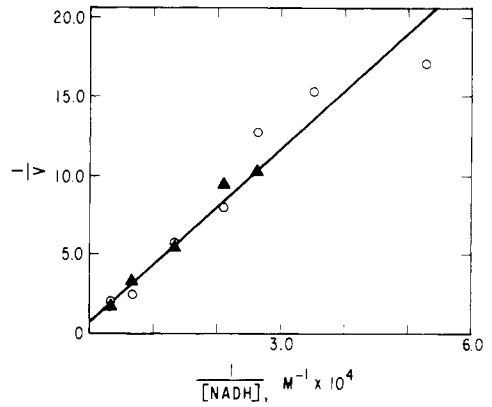

FIGURE 3: The inhibition of yeast alcohol dehydrogenase by borate in sodium pyrophosphate buffer at 25 °C and pH 8.7. (○) 1.9×10^{-5}–3.0×10^{-4} M NADH, 0.01 M acetaldehyde, 0.002 μM enzyme, no borate; (▲) 5.0×10^{-4} M sodium borate.

direction.

YADH-catalyzed ethanol oxidation was studied under rapid mixing conditions. The initial velocities show steady-state kinetic behavior as evidenced by the double-reciprocal plots obtained which are identical with those shown in Figure 1, with identical kinetic parameters. Typical results of the stopped-flow studies are seen in Figure 4. Three premixing conditions were used as follows: (i) syringe 1, NAD^+ and borate, syringe 2, YADH and ethanol; (ii) syringe 1, NAD^+ and ethanol, syringe 2, YADH and borate; (iii) syringe 1, ethanol and borate, syringe 2, NAD^+ and YADH. Depending upon the premixing conditions, various results are observed. These are listed in Table II. In the absence of borate, the steady-state rate obtained when enzyme is premixed with coenzyme (premixing condition (iii)) is about 50% accelerated compared to the other two sets of premixing conditions, (i) and (ii). Under those conditions in which NAD^+ and borate are premixed, no initial burst reaction is observed in contrast to the results obtained when NAD^+ and borate are not premixed. The burst reaction follows first-order kinetics, and the burst height increases with increasing NAD^+ concentration and decreases with increasing borate concentration. Under the conditions used, the NADH produced in the burst reaction is up to ten times the active site concentration.

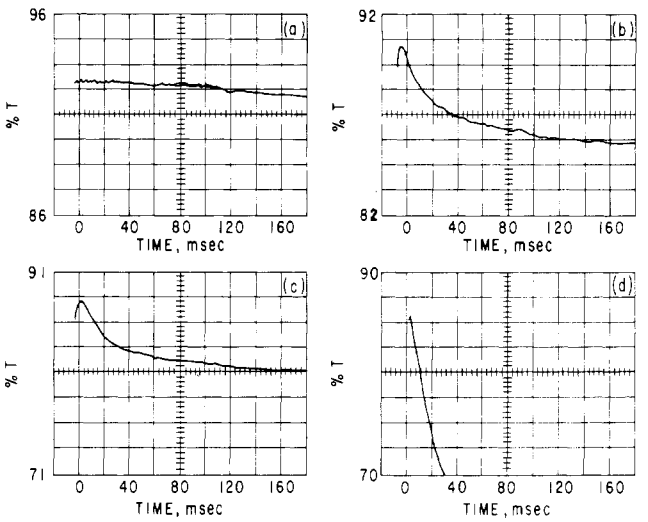

FIGURE 4: Stopped-flow kinetic results at 340 nm for the oxidation of EtOH by NAD^+ with YADH at pH 8.7 under different premixing conditions. (a–c) YADH, 1.8 μM; NAD^+, 0.5 mM; EtOH, 25 mM; sodium borate, 28 mM. (a) NAD^+ premixed with borate, mixing condition i in the Experimental Section; (b) YADH premixed with borate, mixing condition ii; (c) EtOH premixed with borate, mixing condition iii; (d) same as (c), but without borate. The initial transmittance expected from addition of reactant transmittances is ca. 90%.

Discussion

NAD^+ and $NAD\text{-}SO_3^-$ both form complexes with borate, with NAD^+ forming a more stable complex than $NAD\text{-}SO_3^-$ by a factor of 6 (Johnson and Smith, 1976). In view of this fact the most likely scheme to account for the great effect borate has on the equilibrium between ethanol-NAD^+ and acetaldehyde-NADH can be explained by borate entering into the reaction scheme rather than merely altering the catalytic power of the enzyme. This is shown in Scheme I, in which K_I is the intrinsic apparent equilibrium constant defined as $[NADH][AcCHO]/[NAD^+][EtOH]$, constant pH conditions used. The apparent equilibrium constant at pH 8.7, K_{app}, according to Scheme I is given by eq 3. K_{II} and K_{III} are defined as complexation constants with NAD^+ and NADH, respectively, and are given by $[\text{nucleotide-borate}]/[\text{nucleotide}][B(OH)_4^-]$. Solution of eq 3 yields the following values: K_I, 0.0053 ± 0.000016; K_{II}, 2000 ± 60 M^{-1}; K_{III}, 130 ± 8 M^{-1}. The value of K_{II} is identical with the value of boration constant of NAD^+ obtained from the study of the perturbation effect of borate on the NAD^+-sulfite equilibrium system (Johnson and Smith, 1976). The overall equilibrium constant, $[H^+][AcCHO]\cdot[NADH]/[NAD^+][EtOH]$, is equal to $K_I[H^+]$ or 9.4×10^{-12} M. This value is nearly equal to the value of 9.7×10^{-12} M obtained under similar conditions (Bäcklin, 1958).

$$K_{app} = \frac{K_I(1 + K_{III}[B])}{1 + K_{II}[B]} \quad (3)$$

NADH has much less affinity to borate as compared with NAD^+. The ratio of the boration equilibrium constants for NAD^+/NADH is 15, a value which is higher than the ratio of 6 for the boration equilibrium constants for $NAD^+/NAD\text{-}SO_3^-$ (Johnson and Smith, 1976). As proposed earlier the equilibrium constant for boration of nucleosides increases as the electropositive nature of the substituent in the 1 position of ribose increases. For the nicotinamide side chain the following order is observed:

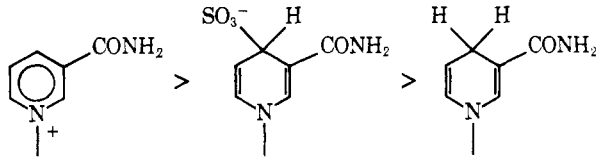

The sulfonate moiety according to this order is more electron withdrawing than the hydrogen moiety. This order follows the order expected according to the Hammet σ_p parameters for sulfonate and hydrogen, 0.09 and 0.00, respectively (McDaniel and Brown, 1958). A ρ value of 4.1 is calculated using the equilibrium constant of 300 M^{-1} for the boration of the NAD-SO_3^-.

The results of the rapid mixing experiments can be understood by viewing the kinetic competition of the enzyme and borate for NAD^+ according to Scheme II. The result-

Scheme II

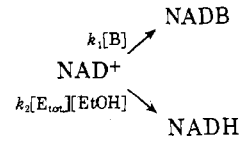

ing kinetic expression is shown in eq 4 where $[E_{tot}]$ is the initial enzyme concentration. When $[NAD^+] \ll K_m$, eq 4 simplifies to an equation which can be integrated to

$$-d[NAD^+]/dt = k_1[B][NAD^+] + k_2[E_{tot}][NAD^+]/(K_m + [NAD^+]) \quad (4)$$

give a pseudo-first-order rate expression (eq 5) for $[NAD^+]_t$, the NAD^+ concentration at any time t. The ratio of the yield of the two products [NADH]/[NADB] at the end of the burst is given by the ratio of the corresponding first-order rate constants $k_2[E_{tot}]/k_1[B]K_m$ (Frost and Pearson, 1965).

$$[NAD^+]_t = [NAD^+]_0 e^{-(k_1[B]+k_2[E_{tot}]/K_m)} \quad (5)$$

The exact eq 5 does not apply here because the initial NAD^+ concentration is not less than K_m. For these conditions, eq 4 must be integrated leading to a complex equation. For the present purposes, eq 5 and the product relationship qualitatively describe the behavior to be expected according to Scheme II. The facts that burst kinetics is observed only when NAD^+ and borate are not premixed and that the magnitude of the burst reaction decreases with increasing borate concentration indicate that Scheme II describes the situation. Borate is expected to react within the time scale of these experiments because NAD-SO_3^- is known to react with borate with rate constants of 350 M^{-1} s^{-1} for the boric acid reaction and 285 M^{-1} s^{-1} for the borate reaction (Johnson and Smith, 1976). The reaction times observed in the burst reactions are consistent with a similar order of magnitude for the NAD^+-borate reaction rate constants.

An interesting aspect of the current problem is that greater burst heights are seen under mixing conditions (iii), NAD^+-enzyme plus borate-ethanol as compared with mixing conditions (ii), enzyme-borate plus NAD^+-ethanol (Table II). Since the initial rate obtained under mixing conditions (iii) in the absence of borate is found to be larger than that of the corresponding mixing conditions (i) and (ii), enzyme activation brought about by coenzyme binding is indicated, giving rise to greater NADH yields in the initial state of the reaction. Luisi and Favilla (1972) have proposed that enzyme activation is likely to be an intramolecular isomerization of coenzyme-enzyme-substrate complex for LADH in the case of NADH binding.

Table II: Kinetic Values for the Oxidation of Ethanol by NAD^+ with Yeast Alcohol Dehydrogenase under Different Premixing Conditions.[a,b]

Kinetic Parameters	[Borate] (mM)	Mixing Conditions[c] i NAD^+ Premixed with Borate	ii YADH Premixed with Borate	iii EtOH Premixed with Borate[d]		
Steady-state rate[e] (M/s × 10^5)	0	30	30	45	80	100
	2.8	4.8	6.4	5.3		
	7.0	1.7	4.0	3.2	5.9	6.4
	28	0.3	0.8	1.1	1.2	1.9
First-order burst rate constant (s^{-1})	2.8		29	16	13	
	7.0		53	28	33	57
	28		69	80	150	120
Burst height (M × 10^5)	2.8		1.7	4.2	8.2	
	7.0		0.7	2.3	4.2	3.3
	28		0.3	0.5	0.7	1.1

[a] Reaction rates and burst height determined by stopped-flow spectrophotometry. [b] Reactions performed at 25 °C in 0.011 M sodium pyrophosphate buffer, μ = 0.1 M, pH 8.7. Concentrations of reagents: NAD^+, 0.50 mM; ethanol, 0.025 M; YADH, 1.8 μM. [c] Mixing conditions: (i) syringe 1, enzyme and ethanol, syringe 2, NAD^+ and borate; (ii) syringe 1, enzyme and borate, syringe 2, NAD^+ and ethanol; (iii) syringe 1, enzyme and NAD^+, syringe 2, ethanol and borate. [d] Data in first column obtained using same reagent concentrations as in footnote *b*. For data in second column, concentration of NAD^+ is 0.0010 M. For third column, concentration of enzyme is 3.5 μM. [e] When there is no burst, the steady-state rate is the initial velocity. When there is a burst, the steady-state rate is the velocity measured shortly after the burst portion of the curve. [f] V_{max}/active site enzyme concentration is equal to 240 s^{-1} (mixing conditions i and ii in Experimental Section) to 450 ± 50 s^{-1} (mixing condition iii), as compared with the value of 500 s^{-1} obtained using similar conditions by Dickenson and Dickinson (1975).

The finding of only steady-state kinetics under the conditions of rapid mixing is in marked contrast to the behavior of LADH-catalyzed ethanol oxidation by NAD^+ (Shore and Gutfreund, 1970), which gives rise to a burst reaction under rapid mixing conditions. The steady-state rate for LADH-catalyzed ethanol oxidation is identical with the rate of NADH dissociation from the enzyme. The burst rate corresponds to the catalytic step in the ternary complex interconversion and gives rise to enzyme-bound NADH. The mechanism of YADH has been deduced to be ordered bi bi by Wratten and Cleland (1963) as a result of product inhibition studies. From a study of the forward and reverse reactions of ethanol and higher alcohol oxidation, Dickenson and Dickinson (1975) concluded that a random mechanism prevails for the formation of the ternary NAD^+-alcohol-YADH complex and an ordered addition prevails for the formation of the ternary NADH-aldehyde-YADH complex. These authors also concluded that the rate-limiting step for ethanol oxidation is the dissociation of NADH from the enzyme under steady-state conditions. Our rapid mixing studies indicate that ternary complex interconversion is rate limiting or at least partially rate limiting. If NADH dissociation is rate limiting under steady-state conditions, a burst reaction should have been observable under the experimental conditions. These results are consistent

with the steady-state isotope effect studies with ethanol and 1,1-dideuterioethanol as substrates (Mahler and Douglas, 1957), where an isotope effect of 1.8 was found for V, a value similar to that found by Klinman (1974) using ethyl-d_5 alcohol as substrate.

In the case of the steady-state kinetics, alternate possibilities for borate inhibition include reaction at the zinc centers of YADH as in the case of LADH (Li et al., 1963). The general scheme is shown in Scheme III and the general

Scheme III

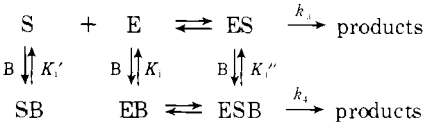

expression for the initial velocity is given by eq 6. Depending upon the relative values of the inhibition constants and the rate constants k_3 and k_4, various kinetic results are expected. When $K_i \ll K_i'$ or vice versa and k_4 is zero the type of inhibition will be of the linear noncompetitive type, a result not observed here. Nor was a hyperbolic noncompetitive type of inhibition observed as predicted by the above scheme when $k_4 \neq 0$. Another possibility is that both YADH and NAD^+ form unreactive complexes with borate, i.e., a double competitive inhibition. This would correspond to Scheme III in which $K_i'' \gg K_i$ or K_i'. This possibility predicts competitive inhibition which contains higher order terms in borate, according to eq 7. However, only linear inhibition was observed for borate concentration up to 0.02 M. Furthermore the values of the inhibition constants for YADH, LDH, and GPDH (the latter two enzymes do not contain zinc) are equal to the inverse of the boration constants for NAD^+. This is consistent with the scheme shown in eq 2a or in Scheme III with K_i', $K_i'' \gg K_i$.

$$v = \frac{(k_3 + k_4[B]/K_i'')[S_{tot}][E_{tot}]}{[S_{tot}](1 + [B]/K_i'') + K_s(1 + [B]/K_i)(1 + [B]/K_i')} \quad (6)$$

$$v = \frac{k_3[S_{tot}][E_{tot}]}{[S_{tot}] + K_s(1 + [B]/K_i)(1 + [B]/K_i')} \quad (7)$$

Borate can interact with enzyme systems and change the overall equilibrium constant of any reaction involving sugars and diols. The large effect observed for the NAD^+ system stems from the great difference in affinity of NAD^+ and NADH for borate, a factor of 15. Borate would be expected to have a large kinetic effect only on those systems in which favorable binding to the substrate exists, for example, a much greater kinetic effect on enzymatic reactions involving NAD^+ as the substrate in contrast to NADH would be expected. The lack of borate inhibition found for lactate dehydrogenase by Misawa et al. (1966) can be explained by the assay used by these authors, i.e., the NADH reduction of pyruvate. It would be expected that at low concentration borate would react most effectively with NAD^+ as compared with other nucleotides because of the requirements of the electropositive groups on the ribose moiety for stabilization of the borate complex.

At higher borate concentrations, i.e., 10^{-2}–10^{-1} M, both NAD^+ and NADH would be entirely complexed and the effect of borate on a biological system would be determined by the less favorable binding sites. An example of this is proposed in the effect of 0.02–0.5 M borate buffer on the reaction of reduced pyridine nucleotides and cytochrome b_5 reductase (Strittmatter, 1964). Borate acts as a nearly competitive inhibitor of the oxidation of NADH. It reverses the electron flow when added to NAD^+ analogues and reduced cytochrome b_5 (a flavoprotein). A replot from the double-reciprocal plot in the paper shows nonlinear higher order inhibition. These results can be explained by Scheme III and eq 6 where $K_i'' \gg K_i$ or K_i'. The higher order inhibition may be due to the $(1 + [B]/K_i)(1 + [B]/K_i')$ term in the denominator of eq 7. At high borate concentrations, reduced and oxidized pyridine nucleotides are both borated, and only the effect of boration of the oxidized vs. reduced flavoprotein is seen. It would be expected that the oxidized flavin nucleotide would bind borate more favorably than reduced flavin in analogy with pyridine nucleotides, and the overall equilibrium in a flavin–nucleotide system would favor reduced pyridine nucleotide and oxidized flavin formation.

In a total biological oxidation–reduction system, low concentrations of borate would be expected to change the oxidation potential of the NAD^+–NADH couple by 0.036 V and hence alter the ability of NAD^+ to oxidize substrates with a higher potential, substrates such as glyceraldehyde phosphate, ferredoxin, and lipoic acid.

Acknowledgment

We are grateful to Mrs. Ingrid Kuo and Ms. Cynthia Solano for assistance in running the gel electrophoresis.

References

Bäcklin, K.-I. (1958), *Acta Chem. Scand. 12,* 1279.
Deitrich, R. A. (1967), *Arch. Biochem. Biophys. 119,* 253.
Dickenson, C. J., and Dickinson, F. M. (1975), *Biochem. J. 147,* 303.
Frost, A. A., and Pearson, R. G. (1965), Kinetics and Mechanism, New York, N.Y., Wiley.
Hayes, J. E., and Velick, S. F. (1954), *J. Biol. Chem. 207,* 225.
Johnson, S. L., and Smith, K. W. (1976), *Biochemistry,* preceding paper in this issue.
Klinman, J. P. (1974), in Alcohol and Aldehyde Metabolizing Systems, Thurman, R. G., Yonetani, T., Williamson, J. R., and Chance, B., Ed., New York, N.Y., Academic Press, p 81.
Li, T. K., Ulmer, D. D., and Vallee, B. L. (1963), *Biochemistry 2,* 482.
Lineweaver, H., and Burk, D. (1934), *J. Am. Chem. Soc. 56,* 658.
Luisi, P. L., and Favilla, R. (1972), *Biochemistry 11,* 2303.
Mahler, H. R., and Douglas, J. (1957), *J. Am. Chem. Soc. 79,* 1159.
McDaniel, D. H., and Brown, H. C. (1958), *J. Org. Chem. 23,* 420.
Misawa, T., Kaneshima, H., and Akagi, M. (1966), *Chem. Pharm. Bull. 14,* 467.
Roush, A., and Gowdy, B. B. (1961), *Biochim. Biophys. Acta 52,* 200.
Roush, A., and Norris, E. R. (1950), *Arch. Biochem. 29,* 345.
Shore, J. D., and Gutfreund, H. (1970), *Biochemistry 9,* 4655.
Strittmatter, P. (1964), *J. Biol. Chem. 239,* 3043.
Theorell, H., and Yonetani, T. (1963), *Biochem. J. 338,* 537.

Vallee, B. L., and Hoch, F. L. (1955), *Proc. Natl. Acad. Sci. U.S.A. 41*, 327.
Weser, U. (1968), *Hoppe-Seyler's Z. Physiol. Chem. 349*, 1479.
Wratten, C. C., and Cleland, W. W. (1963), *Biochemistry 2*, 935.

Osmium(VI) Complexes of the 3′,5′-Dinucleoside Monophosphates, ApU and UpA†

F. Bernard Daniel and E. J. Behrman*

ABSTRACT: The dinucleoside monophosphates, ApU and UpA, react with potassium osmate (VI) and 2,2′-bipyridyl to form the corresponding oxo-osmium(VI) bipyridyl sugar esters in which the osmate group is bonded to the terminal 2′,3′-glycol. Osmium(VIII) tetroxide and 2,2′-bipyridyl react with the dinucleosides to form the corresponding oxo-osmium(VI) bipyridyl heterocyclic esters which result from addition of the tetroxide to the 5,6-double bond of the uracil residue. Although capable of transesterification reactions, these heterocyclic esters are exceptionally stable toward exchange reactions in solution. No apparent exchange was observed after 1 month. This reaction thus seems promising for single-site osmium labeling in polynucleotides.

The chemistry of heavy metal–polynucleotide complexes has important biochemical implications. Certain *cis*-Pt(II) complexes are effective antitumor agents (Rosenberg, 1973; Davidson et al., 1975; Aggarwal et al., 1975). Work on other transition metal complexes should be pursued in this connection (Cleare, 1974). Heavy metal interactions with polynucleotides are interesting in other ways as well (Clarke and Taube, 1974). In particular, oxo-osmium reagents form heavy atom derivatives of polynucleotides which have proved useful for x-ray crystallographic work (Rosa and Sigler, 1974; Suddath et al., 1974; Robertus et al., 1974) and also for the direct visualization approach to the sequencing problem (Salser, 1974; Whiting and Ottensmeyer, 1972).

Oxo-osmium(VI) ligand complexes react with *cis*-glycols to yield the same hexacoordinate monomeric esters which are formed by reaction of the corresponding olefin with an oxo-osmium(VIII) ligand complex (Criegee et al., 1942). The common reactive sites in nucleic acids are the 2′,3′-glycol in a terminal ribose group (Daniel and Behrman, 1975; Conn et al., 1974) for the osmium(VI) reaction and the 5–6 double bond of uracil and thymine residues (Subbaraman et al., 1971; Beer et al., 1966; Highton et al., 1968; Burton, 1967; Burton and Riley, 1966) for the osmium(VIII) system. Osmium(VIII) reagents also oxidize thio bases such as 4-thiouridine (Burton, 1967, 1970) and react rapidly with the isopentenyladenine group (Ragazzo and Behrman, 1976). The interesting chemistry of the reaction discovered by Rosa and Sigler (1974) is not yet clear. The nature of the reaction with olefins is radically affected by the presence of ligands containing tertiary nitrogen such as pyridine. Griffith (Collin et al., 1973, 1974) has shown that in the absence of such ligands, the product is a dimer containing pentacoordinate Os(VI) rather than the tetracoordinate monomer which had been long assumed. The ligand also affects both the rate of formation and the rate of hydrolysis of the product. For example, at pH 9.5, the rate of hydrolysis is increased by about a factor of 30 and the rate of formation decreased by about a factor of 1000 for the ligand-free system as compared with the bis(pyridine) ester (Subbaraman et al., 1972).

We have recently shown (Daniel and Behrman, 1975) that the nature and concentration of ligand species also affect the rate of the ester interchange reaction shown in Figure 1. The rate of the ester interchange reaction is inversely proportional to ligand concentration. For pyridine, the half-time is of the order of minutes. When the ligand is bidentate, however, the half-time for the reaction is greatly increased, particularly in the presence of excess ligand.

All of these factors are of importance for single-site labeling of polynucleotides in aqueous solution; hydrolysis must be prevented and the rate of ester interchange should be minimized. Rosa and Sigler (1974), for example, report that $tRNA^{fMet}$ in solution reacts with both Os(VI) and Os(VIII) species at many sites although only a single site reacts when osmium reagents are allowed to diffuse into crystals. We show in this paper that the 3′,5′ dinucleoside monophosphates UpA and ApU can be selectively labeled with an oxo-osmium(VIII) bipyridyl reagent at the 5–6 double bond of the uracil residue. Exchange to give the sugar ester does not occur to a significant extent.

Results and Discussion

Sugar Esters. Both dinucleoside monophosphates, ApU and UpA, reacted with potassium osmate and 2,2′-bipyridyl to form the expected sugar esters shown in Figure 2A and B. Only one spot was detected by thin-layer chromatography (TLC) in each case. Identification of the product was made by analysis of the low-field nuclear magnetic resonance (NMR) spectra of the products (Figure 3, Table I). The diagnostic resonances are those of the C(1′)-proton for the glycol terminal residue and those of the C(5) and C(6)

† From the Department of Biochemistry, The Ohio State University, Columbus, Ohio 43210. *Received August 12, 1975.* This work was supported by a National Institutes of Health Grant, GM-20375.